Sedimentation in the adjacencies of a southwestern Atlantic giant carbonate ridge

Rosangela Felicio dos Santos[1], Bianca Sung Mi Kim[1], Tailisi Hoppe Trevizani[1], Rodrigo Udenal de Oliveira[1], Mascimiliano Maly[1], Raissa Basti Ramos[1], Rubens Cesar Lopes Figueira[1], Michel Michaelovitch de Mahiques[1,2,*]

[1] Universidade de São Paulo - Instituto Oceanográfico (Praça Oceanográfico, 191 - Butantã - São Paulo - 05508-120 - SP - Brazil)

[2] Universidade de São Paulo - Instituto de Energia e Ambiente (Av. Prof. Luciano Gualberto, 1289 - Butantã - São Paulo - 05508-900 - SP - Brazil)

* Corresponding author: mahiques@usp.br

ABSTRACT

Although carbonate mounds have been investigated for 100 years, few studies focus on the giant variety. The Alpha Crucis Carbonate Ridge (ACCR), a ~17 x 12-km ring-shaped ridge formed by hundreds of mounded structures, located between the 300 and 800-m isobaths and reaching a maximum height of 340 meters above the adjacent seafloor, is the first giant carbonate mounded feature described for the SW Atlantic margin. This study provides the first multiproxy approach to investigate sediments covering the ACCR and its adjacencies. Most of the area is located under the Intermediate Western Boundary Current (IWBC) flow, which carries the nutrient-rich Antarctic Intermediate Water (AAIW). Radiocarbon aging shows pronounced differences for the shallow layers (MIS3 for the top of the mounds and late Holocene for the adjacencies). Grain size data indicate the prevalence of sandy fractions on top of the mounds and muddy sediments in the adjacent areas. Fe/Ca and Ti/Ca proxies allowed for identifying mainly biogenic sedimentation in the area. However, the input of allochthonous terrigenous sediment is necessary for mound buildup, and values of Fe and Ti collected on the top of the mounds are significant. End-Members distributions and metal concentrations also allowed for recognition of distinct sources of sediment. Nd and Ln(Fe/K) indicated two primary terrigenous sources, the Precambrian rocks of the Brazilian shield (Cabo Frio end-member) and the multiple lithologies drained by the Rio de la Plata basin. Redox condition proxies indicated that the area is submitted to oxic conditions, probably reflecting the action of the IWBC. This work provides the first insight into an integrated grain-size and geochemical characterization of the Alpha Crucis Carbonate Ridge (southwestern Atlantic margin).

Descriptors: Carbonate mound, Sedimentation, SW Atlantic, Continental slope.

INTRODUCTION

It has been approximately 100 years since carbonate mounds on the continental slope of the North Atlantic were first described (Joubin, 1922; Teichert, 1958). However, detailed studies on deep-sea carbonate mounds have only been carried out in the last 30 to 40 years, including on gigantic structures (hundreds of meters high, more than one kilometer wide) (Neumann et al., 1977; Akhmetzhanov et al., 2003; Wheeler et al., 2006; Hovland, 2008; Henriet et al., 2014). These features are unique and very vulnerable dominated by framework-building cold-water corals, and their growth reflects the characteristics of the surrounding environment and ocean currents systems (van Weering et al., 2003; Eisele et al., 2008; Steinmann et al., 2020). Deep-sea carbonate mounds are

important not only to coral species but also to the rich and diverse habitat created in these environments (Le Guilloux et al., 2009; D'Onghia et al., 2012; Morigi et al., 2012; Fentimen et al., 2018; Bendia et al., 2021).

Knowledge about buildup, age, evolution, and dynamics is heterogeneous and, sometimes, contradictory. The most detailed information about carbonate mounds is regarding the Porcupine Basin (West of Ireland), characterized by the presence of three mound provinces (Magellan, Hovland, and Belgica) (De Mol et al., 2002; Huvenne et al., 2007). In each of these provinces, the mounds appear under specific conditions and morphology: high mounds up to 200 m (Hovland), buried small mounds with irregular shapes (Magellan), and outcropping and buried conical mounds (Belgica). The internal structures are formed by intercalations of biogenic sands and terrigenous muds (De Mol et al., 2002). The ages of these mounds can be highly variable, and some have been dated up to the end of the Pliocene, with interruption intervals during their development (Dorschel et al., 2005b; Kano et al., 2007; Thierens et al., 2010).

The development of carbonate mounds is attributed either to the seepage of fluids (Hovland, 1990; Mangelsdorf et al., 2011; Suess, 2014), hydrodynamic controls (Wheeler et al., 2006; White, 2006; Correa et al., 2012), or a combination of both (De Mol et al., 2002), sometimes triggered or favored by landslides (De Mol et al., 2008). As such, they can provide essential information regarding surrounding environmental characteristics that might reflect geological mechanisms, hydrodynamic patterns, and the development of biological communities.

The first reports of cold-water corals on the southeastern/southern Brazilian continental slope are attributed to Viana et al. (1998) in the Campos Basin and Sumida et al. (2004) in Santos Basin. Viana et al. (1998) reported carbonate mounds on the outer shelf (up to 120 meters water depth) in Campos Basin. Sumida et al. (2004) found cold-water corals associated with pockmark features that are not active but show evidence of residual gas escape (dos Santos et al., 2018). Other studies deal with the occurrence of deep-sea corals in the Pelotas Basin (Carranza et al., 2012).

Information about giant mounds in the Southern Atlantic is more limited (Maly et al., 2019; Steinmann et al., 2020), with the Alpha Crucis Carbonate Ridge (ACCR) being the first giant carbonate mounded feature described for the SW Atlantic margin (Maly et al., 2019) (Figure 1). The ACCR is a ~17 x 12-km ring-shaped ridge formed by hundreds of mounded structures between the 300 and 800-m isobaths and reaching a maximum height of 340 meters above the seafloor. The most abundant CWC building species in the ACCR are *Desmophyllum pertusum*, *Solenosmilia variabilis*, *Enallopsammia rostrata*, and *Madrepora oculata* (Viana et al., 1998; Sumida et al., 2004; Mangini et al., 2010; Raddatz et al., 2019). These corals play an important ecological role and participate in the ocean carbon cycle, composing vulnerable marine ecosystems that need conservation. They have been considered potential World Heritage sites (UNESCO) due to their importance for global and, more specifically, deep-sea, biodiversity (Freiwald et al., 2004; Roberts et al., 2006; Henriet et al., 2014).

Although several other carbonate mounds have been described, including giant mounds in the North Atlantic (Neumann et al., 1977; Akhmetzhanov et al., 2003; Wheeler et al., 2006; Hovland, 2008; Henriet et al., 2014), the ACCR was the first carbonate mound of such scale reported in the SW Atlantic (Maly et al., 2019). Thus, further study of this carbonate feature is necessary. Despite some similarities, including the cold-water coral species identified as major constituents, the development of such structures is unique as they respond to different climates, ocean current systems, and sediment fluxes compared to terrigenous environments (Dorschel et al., 2005a; Rüggeberg et al., 2005; White, 2006; Dorschel et al., 2007; Eisele et al., 2008; White and Dorschel, 2010).

The sedimentary texture and composition of carbonate mounds and their adjacencies vary (Rüggeberg et al., 2005; van der Land et al., 2014; Terhzaz et al., 2018) depending on several factors such as the contribution of organic and inorganic carbonates (Gischler and Zingeler, 2016), terrigenous supply from adjacent continents and shelves (Dorschel et al., 2005a; Rüggeberg et al., 2007),
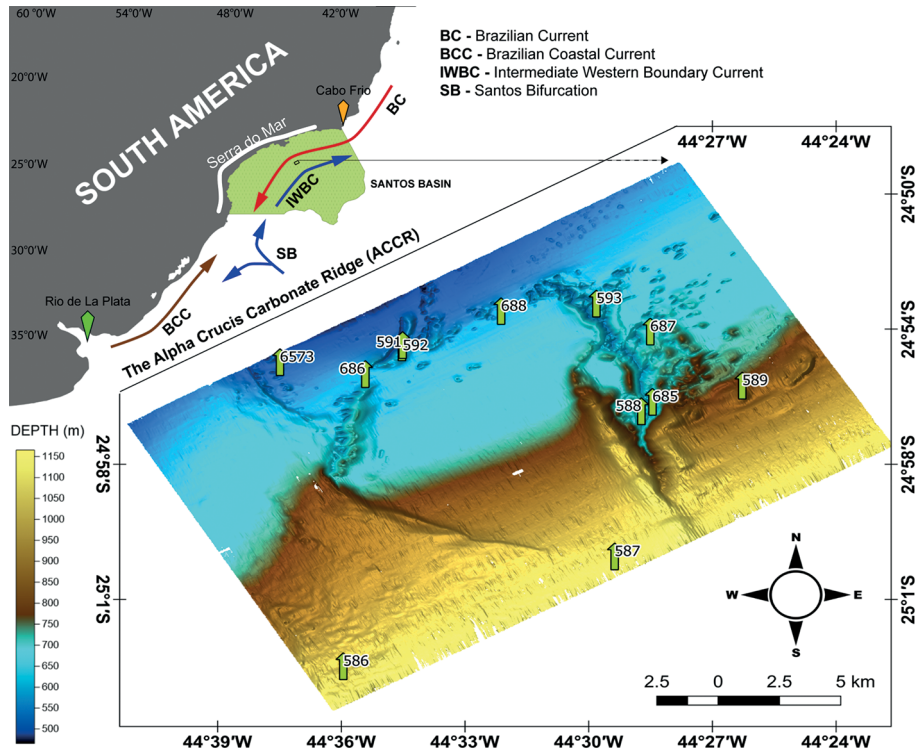
Figure 1. Location of the Alpha Crucis Carbonate Ridge (ACCR) in the context of the Santos Basin. Green arrows present the location of the samples used in this work. The main current systems are shown as colored arrows: Brazil Current (BC - red), Brazilian Coastal Current (BCC - brown), Intermediate Western Boundary Current (IWBC - blue), Santos Bifurcation (SB - blue bifurcation).

and diagenesis (van der Land et al., 2011). Their biogenic components consist mainly of cold-water corals (CWC), *Desmophyllum pertusum,* and *Madrepora oculata* (Freiwald, 2002; Freiwald et al., 2004).

The elemental composition of sediments provides a wide range of information on their sources, past climates, ocean circulation, organic production, redox conditions, and post-depositional changes in sediment sequences (Calvert and Pedersen, 2007). Determining metals and metal/metal ratios in sedimentary columns is a powerful tool for building oceanographic and environmental reconstructions when coupled with a chronological analysis (Moreno et al., 2004). Fe/Ca and Ti/Ca discriminate terrigenous input (Govin et al., 2012). Fe/K is considered a proxy for continental rainfall (Rothwell and Croudace, 2015), Metal/Ca allows for verifying the carbonate origin , Sr/Ca has been used as a proxy for aragonite, and Mg/Ca for calcite (Rothwell and Croudace, 2015). Content variation of elements such as zinc (Zn)

and vanadium (V) in sediment cores can provide important insights into possible changes in the redox state of the sedimentation environment over time (Nameroff et al., 2004).

This work presents the first multiproxy study about sediments covering the ACCR and adjacencies. Grain size, metal concentrations and ratios, and Nd isotope analyses were evaluated to help understand the mechanisms involved in ACCR development. We focused on aspects concerning the Intermediate Western Boundary Current (IWBC) and on the role of fluid seepage in modifying seafloor sediment characteristics. The main goals of the present study are: (i) to identify the redox conditions of the sediment covering the ACCR and adjacencies in order to verify the influence of the IWBC and, more precisely, of the oxygen-rich water mass carried by this ocean current; (ii) to identify terrigenous sedimentation sources based on grain-size, metals, radiocarbon dating, and Nd isotopes analyses; (iii) to recognize the carbonate sediment fractions through the use of metal ratios;

and (iv) to identify the influencing factors supporting carbonate mound development at the ACCR.

STUDY AREA

The ACCR is located in the central part of the São Paulo Bight (Butler, 1970; Zembruscki, 1979), 1979), Santos Basin, between coordinates 24°53'S-24°59'S and 44°27'W-44°37'W, between the 300 m and 800 m isobaths (Maly et al., 2019) (Figure 1). The Santos Basin is a province rich in hydrocarbons (Portilho-Ramos et al., 2018). Recent studies have established a connection between salt diapirism and fluid seepage in the area (Schattner et al., 2016; de Mahiques et al., 2017b; dos Santos et al., 2018). It is known that gas seepage, particularly methane seepage, may promote the development of microbial communities, serving as substrates for forming deep-ocean coral reef structures (Hovland, 1990). The ACCR ridge's shape and location above a giant salt diapir suggest that its origin is related to gas seepage along the faults generated by the salt uplift (de Mahiques et al., 2017b; Maly et al., 2019).

Geographically, the ACCR is located close to the upper limit of the Aptian salt (Late Aptian, 115 - 112 Ma, approximately) in Santos Basin (Mohriak et al., 2008; Jackson et al., 2015). The present morphology of the upper slope of Santos Basin is strongly influenced by the salt tectonics that affected the basin since the Late Cretaceous (Guerra and Underhill, 2012) and is active until today (de Mahiques et al., 2017b; Schattner et al., 2018).

The evolution of Santos Basin comprises a complete sequence of extensional basin environments, from continental to deep-ocean (Nunes et al., 2004), with a maximum thickness of 12 km (Modica and Brush, 2004). Geographic changes in depocenters and sediment starving after the Late Cretaceous (100 - 66 Ma, approximately) are attributed to the uplift of the Serra do Mar coastal mountain chain (Assine et al., 2008; Cogné et al., 2012). Considering that the uplift of Serra do Mar prevents terrigenous sediment influx from the continental areas directly to the Santos margin, the sediment input to the basin originates mainly from bottom currents (Maly et al., 2019; Schattner et al., 2020).

Information about modern sedimentation on the Santos Basin upper slope is still scarce (de Mahiques et al., 2004; de Mahiques et al., 2017a). The low sedimentation rates revealed by radiocarbon dating reflect the strong dynamics led by the Brazil Current (BC) and Intermediate Western Boundary Current (IWBC) (Silveira et al., 2004; Fernandes et al., 2009; de Mahiques et al., 2011). The effectiveness of the IWBC over the upper slope is attested by the presence of seafloor features such as elongated pockmarks (Schattner et al., 2016) and comet marks (Maly et al., 2019). The IWBC carries the oxygen-rich Antarctic Intermediate Water (AAIW), favoring the presence of cold-water-corals (CWC) between the 500 and 1,200 isobaths (Sumida et al., 2004; Barbosa et al., 2020). Studies on the redox conditions of this area are scarce.

METHODS

This work used sediment samples from twelve box cores collected aboard R/V Alpha Crucis over two surveys conducted in January and November 2019 (Figure 1, Table 1). Each core was sliced at intervals of one centimeter until the core bottom, and each slice was frozen onboard to preserve the sample for further analysis and freeze drying in the laboratory, before analysis. Three cores did not sufficiently penetrate the sedimentary column, and only the coretops were analyzed.

We selected approximately 10 milligrams of specimens of the planktonic foraminifera *Globigerinoides ruber* pink + white and *Globigerinoides sacculifer* from four samples for radiocarbon dating. *Globigerinoides ruber* and *Globigerinoides sacculifer* are widely used as dating materials due to their abundance and ubiquity. The radiocarbon analyses were performed at the Beta Laboratories (Miami, USA). Conventional ages were calibrated using software Calib, version 8.2 (Stuiver et al., 2021), applying a regional reservoir effect (ΔR) of 28±52 years (Alves et al., 2015) and the Marine20 calibration (Heaton et al., 2020).

Grain-size and metal content analyses were conducted for the whole cores. εNd radiogenic isotope analyses were performed only for coretop samples. We also used the εNd value of the

Table 1. Geographic coordinates, water depth, and recovery of the box cores used in this study.

Sample	Latitude (o)	Longitude (o)	Water Depth (m)	Recovery (cm)	Relative Location
586	-25.050	-44.599	1009	41	Out
587	-25.001	-44.490	1070	38	Out
588	-24.937	-44.479	663	32	Top
589	-24.925	-44.438	780	35	Out
590	-24.957	-44.585	650	30	Out
591	-24.908	-44.576	547	Coretop	Top
592	-24.907	-44.575	535	20	Top
593	-24.889	-44.497	563	Coretop	Top
685	-24.932	-44.473	551	Coretop	Top
686	-24.900	-44.474	560	24	Top
687	-24.892	-44.536	530	22	Top
688	-24.920	-44.590	530	18	Top
6573	-24.915	-44.625	501	28	Out

surface sample from a box-core (6573) collected in 2002 aboard R/V Prof W. Besnard, published initially in de Mahiques et al. (2004).

The grain-size distribution of the terrigenous fraction was determined in sediment samples after removing the calcium carbonate fraction with a solution of 10% HCl, eliminating organic matter with a solution of 30% hydrogen peroxide and adding a solution of 20% sodium hexametaphosphate. Each sample was analyzed with a Malvern Mastersizer 2000 Laser Analyzer. Results were recorded at intervals of $1/4\phi$ for muds (finer than 62.5 μm) and $1/2\phi$ for sands. Grain size statistics were computed using the Gradistat macro for MS-Excel (Blott and Pye, 2001). The grain size results were used to determine end-members (Weltje, 1997), using the BasEMMA macro for MS-Excel (Zhang et al., 2020).

Metals (Al, Ca, Fe, K, Mg, Mn, Ti, Ba, Cr, Cu, Ni, Sc, Sr, V, and Zn) were analyzed in Varian 710 Inductively Coupled Plasma Optical Emission Spectrometry (ICP-OES) after total digestion of bulk sediments, using the EPA3052 method (USEPA, 1996), optimized by the use of a DGT 100 Plus digester (Provecto Analítica). Approximately 0.25 g of dry sediment was weighed and inserted in a Teflon digestion tube with 10mL of concentrated HNO_3. The mixture was subjected to microwave digestion for 20 minutes. Then, 2 to 5 mL of 40% HF was added, and the digestion procedure was

repeated. Finally, 1 mL of 30% H_2O_2 was added, and the digestion procedure was repeated. The solution was then filtered through Whatman filters. The filtrate was transferred to a Teflon beaker and heated on a hot plate until evaporation. Then, 20 mL of 5% HNO_3 was added three times and evaporated, and the remnant residue was transferred to a 50 mL flask with distilled water, and the solution was analyzed by ICP-OES. Quality control was evaluated using certified reference material SS-2 (EnviroMAT Contaminated Soil from SCP science), subjected to the same analytical procedure. Results for all elements presented accuracy (recoveries between 78.3%-102.8% with the confidence interval in the certified) and precision (relative standard deviation below 20% (n = 7)) (Porevsky et al., 2014; Lindholm-Lehto et al., 2020) (Supplementary Material 1; https://doi.org/10.5281/zenodo.6967105). Metal/Metal ratios are presented in their natural logarithm (ln) form, following the recommendations of Aitchison and Egozcue (2005) and to facilitate the comparison with the results from Govin et al. (2012).

The Nd isotopic analyses of the non-carbonatic fraction were carried out at the Geochronological Research Centre of the University of São Paulo, Brazil. The Nd analyses, here reported as εNd values, were prepared by standard methods using the analytical procedures described by Sato et al. (1995) and Magdaleno et al. (2017), performed on

a Thermo Neptune Plus ICP-MS. In a microwave oven, the samples were decarbonated with HCl and dissolved with HF, HNO3, and HCl acids. No visible solid residues should be observed after dissolution, and samples with incomplete dissolution were discarded. Nd was then separated using Ln resin (EIChroM Industries Inc.).

The parameter εNd was calculated as follows:

$$\varepsilon Nd = (((^{143}Nd/^{144}Nd_{sample})/(^{143}Nd/^{144}Nd_{CHUR}))-1) * 10^4,$$

where $^{143}Nd/^{144}Nd_{CHUR}$ = 0.512638 (Jacobsen and Wasserburg, 1980).

Statistical analyses were performed using Past (Palaeontological Statistics), version 4.07 (Hammer et al., 2001).

RESULTS

We present all results in Tables 2 (Radiocarbon dating) and in the Supplementary Material files (https://doi.org/10.5281/zenodo.6967105). Photos of selected box cores are available in Supplementary Material 2. The general aspect of the box-core materials was diverse. Samples collected atop mounds are essentially sandy, with high amounts of living and dead corals (samples 685 and 687 in Supplementary Material 2). On the other hand, samples collected in the adjacent areas were muddy, showing a centimeter-thick yellowish-brown centimetric oxidized layer on top of gray sediments (samples 686 and 688 in Supplementary Material 2).

The radiocarbon ages (Table 2) had a wide range, covering the Marine Isotope Stage 3 (34,780 cal BP at 31 cm of sample 588, located at the top of the ridge) to the late Holocene (2,355 cal BP at 40 cm of sample 586 and 3,050 cal BP at 34 cm of sample 589, both located within the vicinity of the ridge). Sample 587, also located near the mound, provided a calibrated age of 9,860 (early Holocene) at 37 cm.

The grain size results (Supplementary Material 3 and 4) reveal that the sediments consisted of unimodal to trimodal, poorly sorted, fine to medium silt, with a mean grain size varying from 7.0 μm (7.1 ϕ) to 27.0 μm (5.2 ϕ). The percentage of sand varies from 0.6%-15.0%, and clays range from 2.8%-8.2%.

Considering the variation of R^2 (Figure 2A), we used a model with three end-members as representative of the grain-size populations since EM3 was the first end-member to reach more than 95% of explained variance ($R^2 > 0.95$). The grain-size modes of each EM are located at 62.5 μm (EM1; 4.00 ϕ), 52.6 μm (EM2; 4.25 ϕ), and 15.6 μm (EM3; 6.00 ϕ) (Figure 2B). The vertical variation of the EMs along with the cores is shown in Figure 3. EM1 (sandy fraction) prevails in samples collected atop the mound (samples 686, 687, and 688), while EM2 (coarse silt) and EM3 (medium to fine silt) are more evident in the samples collected outside the mound area.

The results of metal concentrations are shown in Supplementary Material 5. As a rule, Ca is the most abundant measured element, with concentrations ranging from 25,162 to 112,213 mg kg^{-1}. All samples showed more Ca than Fe (11,247 to 31,223 mg kg^{-1}), and only 11 of 106 samples presented less Ca than Al (4,810 to 60,262 mg kg^{-1}). High values of Ca were found in cores 588, 592,

Table 2. Radiocarbon results of planktonic foraminifera tests of four box cores. Conventional ages were calibrated using a regional reservoir effect (ΔR) of 28±52 years (Alves et al., 2015) and the Marine20 calibration (Heaton et al., 2020).

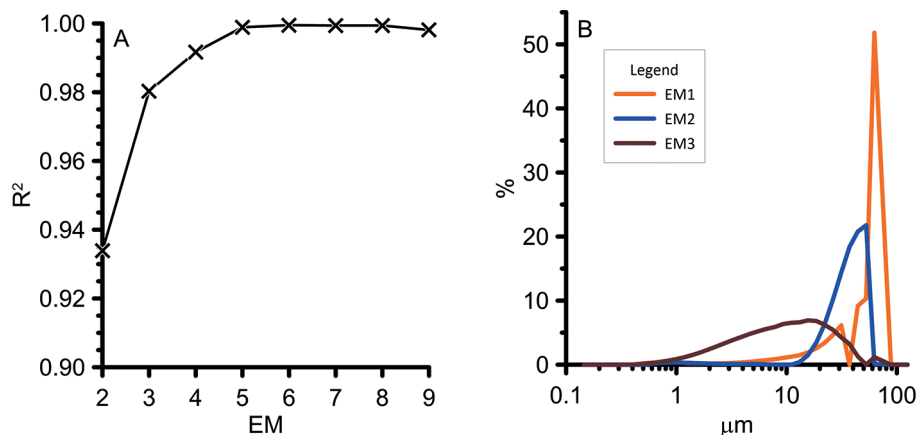| Lab Code	Sample ID	Sediment depth (cm)	Conventional Radiocarbon Age	$\delta^{13}C$ (‰)	Median (Cal BP)	95% interval (Cal BP)	$\Delta^{14}C$ (‰)
Beta 569032	588	31-32	31,210±160	1.6	34,780	34,410 - 35,190	-979.63±0.41
Beta 569033	589	34-35	3,400±30	1.5	3,050	2,835 - 3,265	-350.61±2.45
Beta 569034	587	37-38	9,290±40	1.3	9,860	9,600 - 10,125	-688.06±1.57
Beta 569035	586	40-41	2,820±30	1.0	2,355	2,135 - 2,600	-301.99±2.63

Figure 2. A. Plot of EM versus R2 resulting from the end-member analysis. The analysis with three end-members is the first to reach an explained variance higher than 95%. B. Relative frequency of grain size results in the identification of three-grain size end-members with modes at 62.5 μm (EM1; 4.00ϕ), 52.6 μm (EM2; 4.25ϕ), and 15.6 μm (EM3; 6.00ϕ).

and 593, corresponding to the samples atop the mounds. Values of ϵNd ([Supplementary Material 6](#)) varied between -13.7 and -10.6, indicating a slight variability in Nd isotopic characteristics.

DISCUSSION

GEOCHRONOLOGY AND GENERAL CHARACTERISTICS OF SEDIMENTATION

The number of radiocarbon datings hinders the determination of reliable sedimentation rates for the cores. Two cores (586 and 589) collected outside of the mound area presented late Holocene ages at the base, while the core collected atop the mound (588) provided a Marine Isotope Stage 3 (MIS3) age at 31 cm of core depth. The fourth core presented an early Holocene age at 37-38 cm. These relatively old ages close to the coretops can be attributed either to the high current speeds of the IWBC (Biló et al., 2014) or the turbulent flow occurring at the flanks of mounded structures (Schattner et al., 2018), both consistent with the coarsest grain-size end-member recognized there. According to Biló et al. (2014), the IWBC flow can reach velocities of 30 cm s^{-1}, strong enough to prevent fine fraction deposition. Comet marks, identified by Maly et al. (2019), also indicate the prevalence of intensified flow in the area. These pieces of evidence are suggestive of bypass, or even erosion, on core tops. Kenyon et al. (2003) and Mienis et al. (2009) have recognized high current speeds atop carbonate mounds from

the northeast Atlantic, where currents prevent the burial of coral mounds and ensure food supply to the local fauna. It is worth noting that some of the world's mounds may have a long growth history that exceeds the whole Quaternary. Kano et al. (2007) identified a 2.6 Ma basal age for the Challenger Mound (Ireland margin). Pirlet et al. (2011) identified significant changes in the mound growing in the same area within a much shorter time, including a lack of coral growth.

The sedimentation in the ACCR area is mainly biogenic, with ln(Fe/Ca) and ln(Ti/Ca) below 0 in all samples (Figure 4). There is a higher terrigenous contribution gradient towards the ridge margins and beyond, especially in samples 586 and 587.

Terrigenous sediments are also important constituents for the mounds (Pirlet et al., 2011) and may represent over 50% of a mound's framework (Titschack et al., 2009). The input of allochthonous sediment is necessary for mound buildup (van der Land et al., 2014), as observed in the values of Fe and Ti.

RELATIONSHIP BETWEEN END-MEMBERS (EM) AND METALS

To establish a relationship between grain-size end-members and metals, we performed a Principal Component Analysis (PCA) based on the correlation matrix of these parameters. The scatter plot of the two first principal components
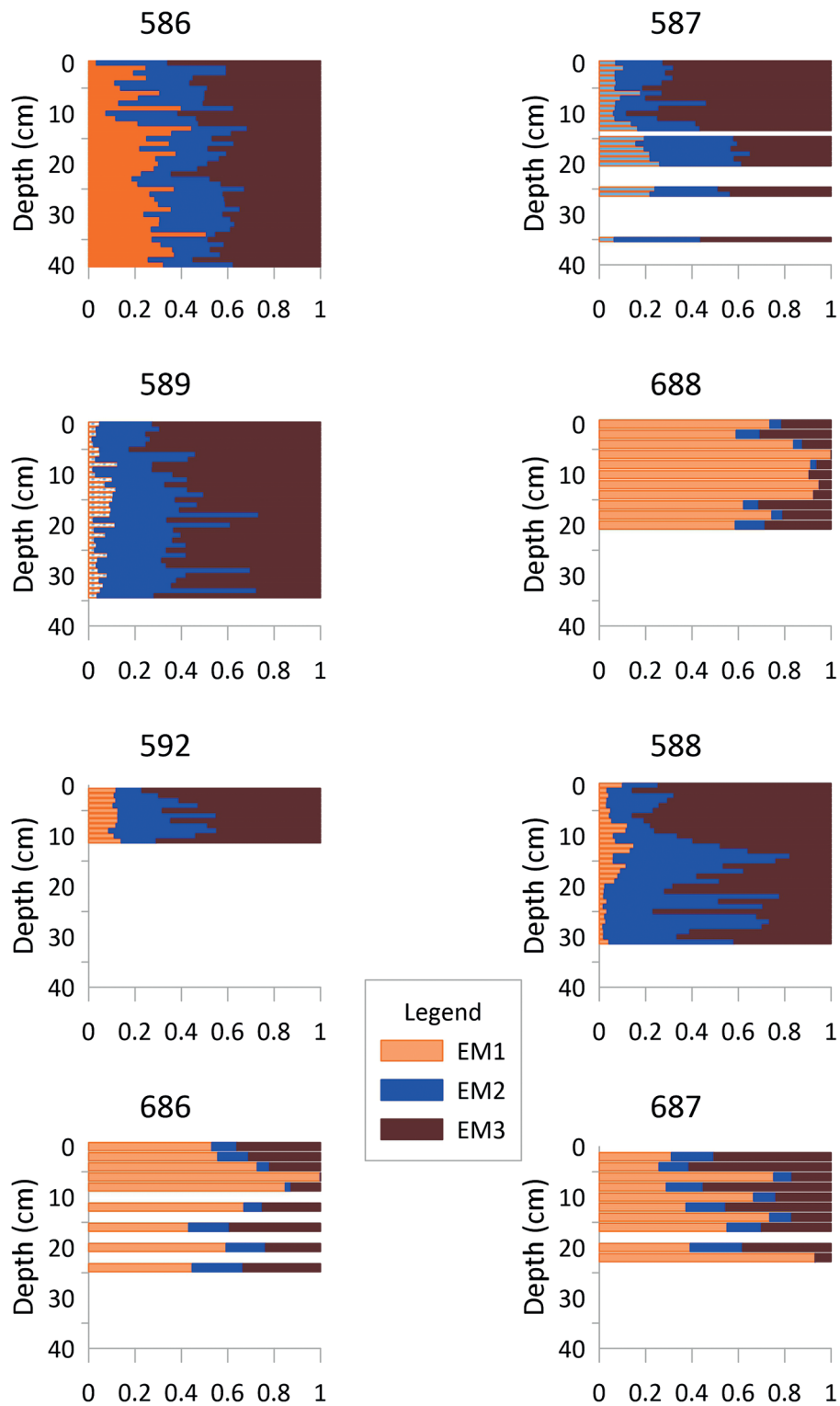
Figure 3. Vertical variations of the end-member relative frequencies along with selected cores from the study area.
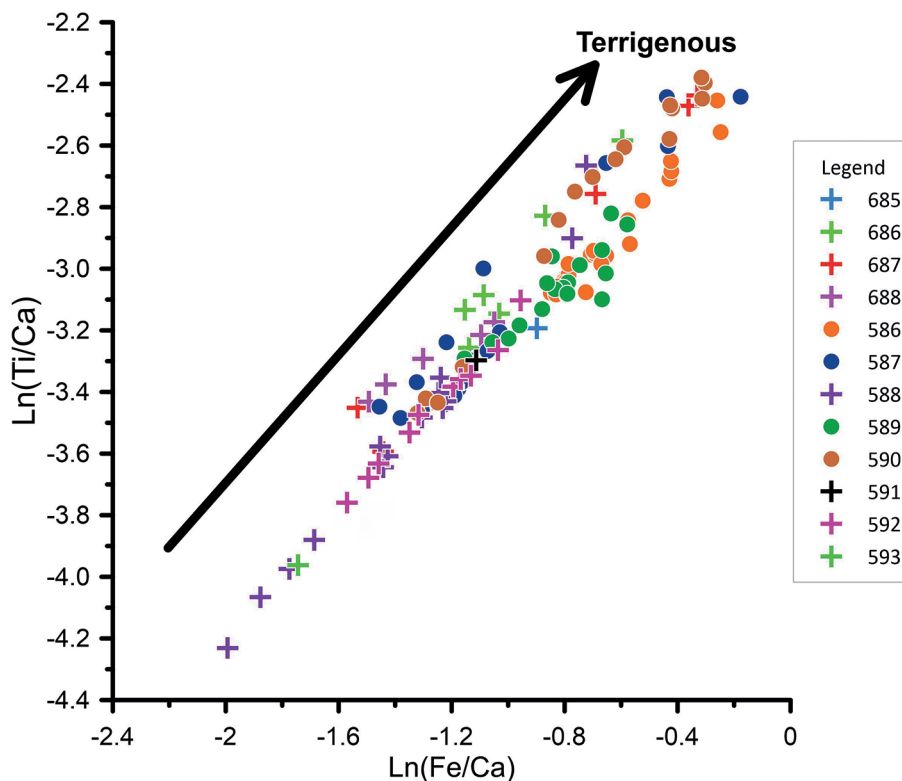
Figure 4. Scatter plot of the natural logarithms of Fe/Ca and Ti/Ca, indicating the linear association between the two ratios and their incidence in a negative range of values. Mound samples are marked as crosses, and out-of-mound samples are marked as dots.

represents 57.75% of the total variance (PC1 = 39.68%, PC2 = 18.07%) (Figure 5). It shows a conspicuous association between EM1 (sandy fraction) with elements present in the biogenic fraction, such as Ca, Sr, Ba, and Mg. It is plausible to admit that the mounds' erosion is a potential source of the sediments presenting that grain-size population. Dorschel et al. (2005b) and Frank et al. (2009) reported phases of erosion of carbonate mounds of the NE Atlantic. In the case of the ACCR, the winnowing action of the high-velocity flow of the IWBC (Legeais et al., 2013; Biló et al., 2014) is noticeable, as observed by the occurrence of "comet marks" associated with small mounds (Maly et al., 2019).

EM3 (finer fraction) presents affinity with copper, an indicator of organic matter input (Tribovillard et al., 2006; Tribovillard, 2021), and manganese, usually associated with the terrigenous fraction (Wagreich and Koukal, 2020). It is worth noting that the terrigenous fraction is an essential

constituent in carbonate mounds (Richter et al., 2006; Pirlet et al., 2011; Terhzaz et al., 2018) and may represent over 50% of the mounds' framework (Titschack et al., 2009). The association of the finer grain-size fraction with the terrigenous input might be explained by the long distance of the potential sources of coarse grains (Mantovanelli et al., 2018; de Mahiques et al., 2021).

Finally, EM2 did not show any association with metals. Nevertheless, since Si was not measured, we cannot discard that this end-member is more associated with the quartzose fraction.

SOURCE OF THE TERRIGENOUS FRACTION AND REDOX CONDITIONS

We used the values of Fe/K and εNd to evaluate potential sources of the terrigenous fraction. Our samples were compared with end-member values assumed for the Río de la Plata, southward of the study area, and Cabo Frio, representing the northern boundary of Santos Basin. These data
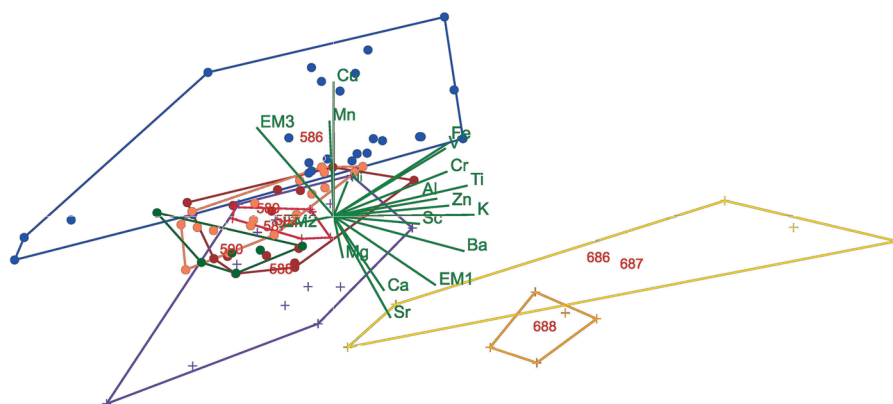
Figure 5. Scatter plot of the two first components from the PCA, representing 57.75% of explained variance, using the results of end-members and metals.

are available in Depetris et al. (2003), Govin et al. (2012), Razik et al. (2015), Mantovanelli et al. (2018), and de Mahiques et al. (2021).

The scatter plot of εNd versus Ln(Fe/K) (Figure 6) shows that, concerning εNd, the samples of the ACCR lie between the values of the Cabo Frio and Río de la Plata end-members and present values of Ln(Fe/K) of the same order of magnitude as the potential sources. In this sense, we admit that the terrigenous fraction of the ACCR ridge presents two primary sources, the Pre-Cambrian rocks of the Brazilian shield (Cabo Frio end-member) and the multiple lithologies drained by the Rio de la Plata basin, including Andean volcanic rocks, Mesozoic basalts, and sedimentary rocks of the Paraná Basin (Mantovanelli et al., 2018). A possible mechanism for the input of sediments from the Río de La Plata to the southern Brazilian slope is provided by Razik et al. (2015) and involves the displacement of Plata Plume Water (Piola et al., 2005) by the Brazilian Coastal Current (Souza and Robinson, 2004) and the capture of the sediments by the Brazil Current (Schattner et al., 2020).

Redox conditions can be evaluated using Metal/Al ratios of selected elements, such as V, Zn, Cu, and U (Morford et al., 2001; Martinez-Ruiz et al., 2015). These elements are commonly used as geochemical proxies that allow inferring redox conditions of marine sediments. For the ACCR, we used the scatter plot of Ln(V/Al) versus Ln(Zn/Al) to analyze the trend of oxic to sub-oxic conditions in the study area (Figure 7). As a rule, most of the samples show values of Ln(Zn/Al) and Ln(V/Al) smaller than -6.0, indicating that the area is submitted to oxic conditions (Martinez-Ruiz et al., 2015), probably reflecting the action of the IWBC. The presence of sandy sediments atop the mounds and the yellowish-brown core-top layers in the muddy sediments also confirms the role played by the energetic intermediate flow in the water depth interval of the study area (Biló et al., 2014). Less oxic conditions are observed in a few samples outside of the ACCR. The concentration of the coral mounds in the zone under the action of the IWBC confirms the importance of hydrodynamics in controlling the development of the mounds, since the IWBC is the leading carrier of the nutrient-rich AAIW in the SW Atlantic margin (Suzuki et al., 2015; Perassoli et al., 2020). This finding follows other studies that report a correlation between deep-sea corals with the action of the AAIW (Thiagarajan et al., 2013; Bostock et al., 2015).

CHARACTERISTICS OF THE CARBONATE FRACTION

Figure 8 presents the scatter plot of Sr/Ca versus Mg/Ca in the sediments. Most samples show high Mg-Calcite, with a clear range towards higher Sr/Ca. This trend is typical of aragonitic carbonate phases, compatible with the composition of deep-sea corals, especially Desmophyllum pertusum (Mikkelsen et al., 1982; Cohen et al., 2006). High-Mg calcite in authigenic concretions is frequently associated with methane seepages (Wehrmann et al., 2011; Suess, 2014; Çağatay et al., 2018),
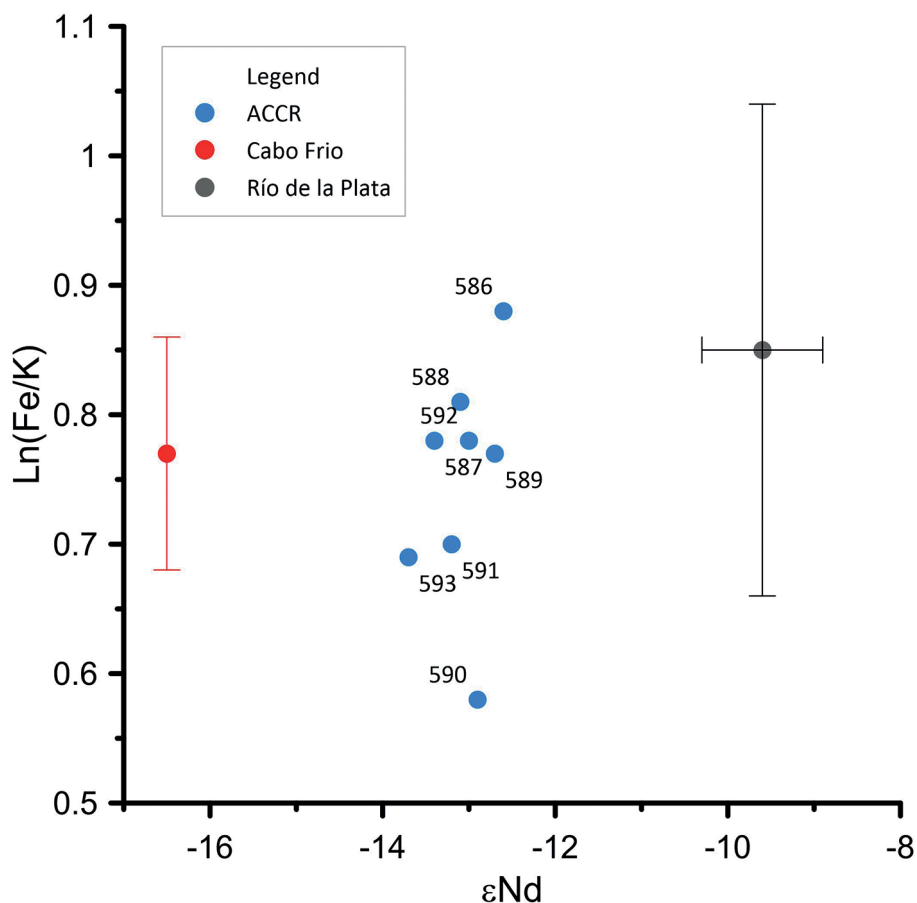
Figure 6. Scatter plot of εNd versus Ln(Fe/K). Red and grey dots correspond to the end-member values of Cabo Frio and Río de la Plata, respectively. Blue dots correspond to the samples collected in the adjacencies of the ACCR.

but this cannot be confirmed in our case since the analyses were performed on bulk sediment samples. Nevertheless, dos Santos (2018) reports the prevalence of high-Mg calcite in a pockmark area on the slope of Santos Basin, confirming the local relationship between the carbonate with gas escape areas. Also, the association of the carbonate mounds of the ACCR with seepage activity was already observed by Maly et al. (2019). It is worth noting that the less aragonitic samples correspond to those located farther from the ridge (i.e., 586, 587, and 589).

CONCLUSION

This work provides the first integrated grain-size and geochemical characterization of the Alpha Crucis Carbonate Ridge (southwestern Atlantic margin). The ages obtained for the

base of four cores suggest the prevalence of low sedimentation rates or winnowing caused by the high speed of the Intermediate Western Boundary Current. This current can also be responsible for maintaining the oxic conditions of the seafloor.

The integration of data allowed for the association between grain size and metal contents. The coarsest sandy fraction is associated with biogenic elements, such as Ca, Ba, Sr, and Mg, and is interpreted as the response to the erosion of the carbonate mounds. The finest end-member was associated with Cu and Mn, related to organic matter and terrigenous sediment input. The intermediate end-member was associated with the quartzose silty fraction.

The source of the terrigenous fraction corresponds to the mixture of two distinct sources,
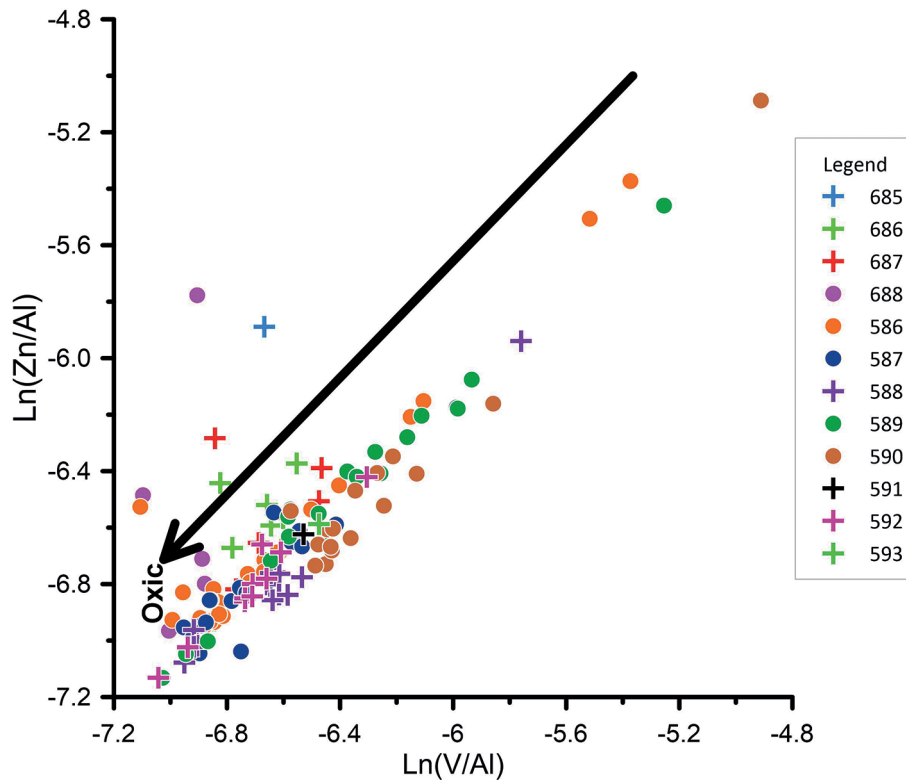
Figure 7. Scatter plot of Ln(V/Al) versus Ln(Zn/Al), indicating the linear association between the two ratios and their low values. Mound samples are marked as crosses, and out-of-mound samples are marked as dots.
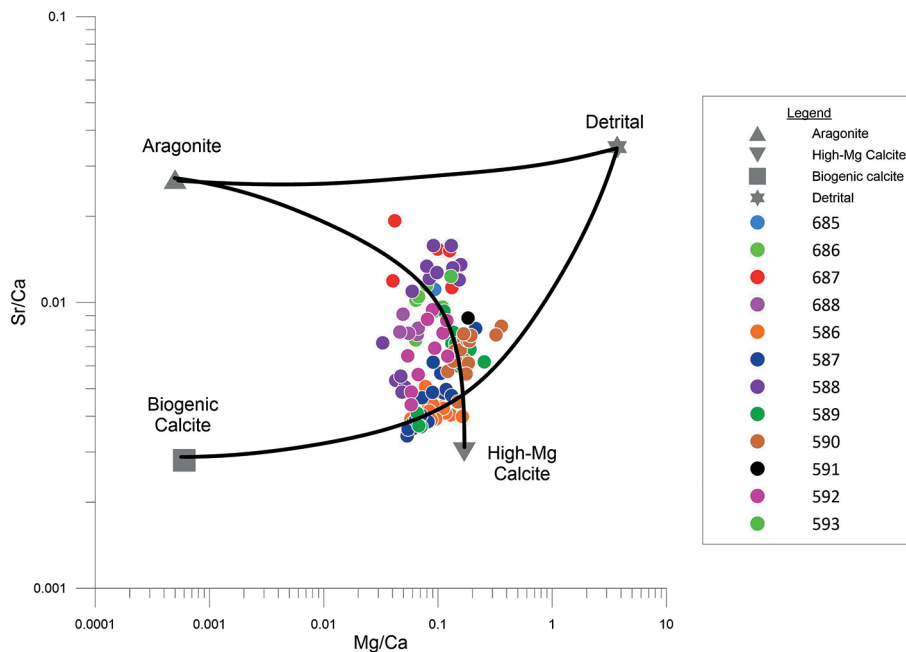

Figure 8. Scatter plot of Mg/Ca versus Sr/Ca. The end-members of the biogenic calcite, high-Mg calcite, aragonite, and detrital fraction are based on Bayon et al. (2007).

the southerly sediments from the Río de la Plata basin and the materials from the Pre-Cambrian shield to the North. Finally, the carbonate fraction is composed of aragonite as a function of the prevalence of corals in the area. The Alpha Crucis Carbonate Ridge is a privileged example of the interaction between intense hydrodynamics and carbonate mounds in the southwestern Atlantic margin.

ACKNOWLEDGMENTS

AUTHOR CONTRIBUTIONS

R.F. dos S.: Methodology; Formal Analysis; Investigation; Writing - original draft; Revision;

B.S.M.K.: Methodology; Formal Analysis; Investigation; Writing - original draft; Revision;

T.H.T: Methodology; Formal Analysis; Investigation; Writing - original draft; Revision;

R.U. de O.: Formal Analysis; Investigation; Writing - original draft; Revision;

M.M.: Formal Analysis; Investigation; Writing - original draft; Revision;

R.B.R.: Project Administration; Formal Analysis; Investigation; Writing - original draft; Revision;

R.C.L.F.: Project Administration; Funding Acquisition; Writing - original draft; Revision;

M.M. de M.: Conceptualization; Project Administration; Funding Acquisition; Investigation; Writing - original draft; Revision.

REFERENCES

AITCHISON, J. & EGOZCUE, J. J. 2005. Compositional data analysis: where are we and where should we be heading? *Mathematical Geology,* 37, 829-850.

AKHMETZHANOV, A. M., KENYON, N. H., IVANOV, M. K., WHEELER, A. J., SHASHKIN, P. V. & VAN WEERING, T. C. E. 2003. Giant carbonate mounds and current-swept seafloors on the slopes of the southern rockall trough. *In:* MIENERT, J. & WEAVER, P. (eds.). *European margin sediment dynamics*. Heidelberg: Springer, pp. 203-209.

ALVES, E., MACARIO, K., SOUZA, R., PIMENTA, A., DOUKA, K., OLIVEIRA, F., CHANCA, I. & ANGULO, R. 2015. Radiocarbon reservoir corrections on the Brazilian coast from pre-bomb marine shells. *Quaternary Geochronology,* 29, 30-35.

ASSINE, M. L., CORRÊA, F. S. & CHANG, H. K. 2008. Migração de depocentros na Bacia de Santos: importância na exploração de hidrocarbonetos. *Revista Brasileira de Geociências,* 38(2), 111-127.

BARBOSA, R. V., DAVIES, A. J. & SUMIDA, P. Y. G. 2020. Habitat suitability and environmental niche comparison of cold-water coral species along the Brazilian continental margin. *Deep Sea Research Part I: Oceanographic Research Papers,* 155, 103147.

BENDIA, A. G., SIGNORI, C. N., NAKAMURA, F. M., BUTARELLI, A. C. A., PASSOS, J. G., RAMOS, R. B., SOARES, L. F., MAHIQUES, M. M., SUMIDA, P. Y. G. & PELLIZARI, V. H. 2021. Microbial perspective on the giant carbonate ridge Alpha Crucis (Southwestern Atlantic upper slope). *FEMS Microbiology Ecology,* 97(8), fiab110, DOI: https://doi.org/10.1093/femsec/fiab110

BILÓ, T. C., SILVEIRA, I. C. A., BELO, W. C., CASTRO, B. M. & PIOLA, A. R. 2014. Methods for estimating the velocities of the Brazil Current in the pre-salt reservoir area off southeast Brazil (23∘ S-26∘ S). *Ocean Dynamics,* 64, 1431-1446.

BLOTT, S. J. & PYE, K. 2001. GRADISTAT: a grain size distribution and statistics package for the analysis of unconsolidated sediments. *Earth Surface Processes and Landforms,* 26, 1237-1248.

BOSTOCK, H. C., TRACEY, D. M., CURRIE, K. I., DUNBAR, G. B., HANDLER, M. R., MIKALOFF FLETCHER, S. E., SMITH, A. M. & WILLIAMS, M. J. M. 2015. The carbonate mineralogy and distribution of habitat-forming deep-sea corals in the southwest pacific region. *Deep Sea Research Part I: Oceanographic Research Papers,* 100, 88-104.

BUTLER, L. W. 1970. Shallow structure of the continental margin, Southern Brazil and Uruguay. *Geological Society of America Bulletin,* 81(4), 1079-1096.

CALVERT, S. & PEDERSEN, T. F. 2007. Elemental proxies for palaeoclimatic and palaeoceanographic variability in marine sediments: interpretation and application. *In:* HALLAIRE-MARCEL, A. V. C. (ed.). *Proxies in Late Cenozoic Paleoceanography.* Amsterdam: Elsevier, pp. 567-644.

CARRANZA, A., RECIO, A. M., KITAHARA, M., SCARABI-NO, F., ORTEGA, L., LÓPEZ, G., FRANCO-FRAGUAS, P., MELLO, C., ACOSTA, J. & FONTAN, A. 2012. Deep-water coral reefs from the Uruguayan outer shelf and slope. *Marine Biodiversity,* 42, 411-414.

COGNÉ, N., GALLAGHER, K., COBBOLD, P. R., RIC-COMINI, C. & GAUTHERON, C. 2012. Post-breakup tectonics in southeast Brazil from thermochronologi-cal data and combined inverse-forward thermal his-tory modeling. *Journal of Geophysical Research: Solid Earth,* 117(B11), B11413.

CORREA, T. B. S., EBERLI, G. P., GRASMUECK, M., REED, J. K. & CORREA, A. M. S. 2012. Genesis and morphology of cold-water coral ridges in a unidirectional current regime. *Marine Geology,* 326-328, 14-27.

D'ONGHIA, G., MAIORANO, P., CARLUCCI, R., CAPE-ZZUTO, F., CARLUCCIO, A., TURSI, A. & SION, L. 2012. Comparing deep-sea fish fauna between coral and non-coral "megahabitats" in the Santa Maria di Leuca cold-water coral province (Mediterranean Sea). *PLoS One,* 7(9), e44509.

DEPETRIS, P. J., PROBST, J. L., PASQUINI, A. I. & GAIE-RO, D. M. 2003. The geochemical characteristics of the Paraná River suspended sediment load: an initial as-sessment. *Hydrological Processes,* 17(7), 1267-1277.

DORSCHEL, B., HEBBELN, D., FOUBERT, A., WHITE, M. & WHEELER, A. J. 2007. Hydrodynamics and cold-wa-ter coral facies distribution related to recent sedimentary processes at Galway Mound west of Ireland. *Marine Ge-ology,* 244, 184-195.

DORSCHEL, B., HEBBELN, D., RÜGGEBERG, A. & DULLO, C. 2005. Carbonate budget of a cold-water coral carbonate mound: Propeller Mound, Porcupine Seabight. *International Journal of Earth Sciences,* 96(1), 73-83.

DORSCHEL, B., HEBBELN, D., RÜGGEBERG, A., DULLO, W. & FREIWALD, A. 2005. Growth and erosion of a cold-water coral covered carbonate mound in the North-east Atlantic during the Late Pleistocene and Holocene. *Earth and Planetary Science Letters,* 233(1-2), 33-44.

EISELE, M. H., HEBBELN, D. & WIENBERG, C. 2008. Growth history of a cold-water coral covered carbonate mound — Galway Mound, Porcupine Seabight, NE-At-lantic. *Marine Geology,* 253(3), 160-169.

FENTIMEN, R., RÜGGEBERG, A., LIM, A., KATEB, A. E., FOUBERT, A., WHEELER, A. J. & SPEZZAFERRI, S. 2018. Benthic foraminifera in a deep-sea high-energy environment: the Moira Mounds (Porcupine Seabight, SW of Ireland). *Swiss Journal of Geosciences,* 111(3), 561-572.

FERNANDES, A. M., SILVEIRA, I. C. A., CALADO, L., CAMPOS, E. J. D. & PAIVA, A. M. 2009. A two-layer approximation to the Brazil Current-Intermediate West-ern Boundary Current System between 20°S and 28°S. *Ocean Modelling,* 29(2), 154-158.

FRANK, N., RICARD, E., LUTRINGER-PAQUET, A., VAN DER LAND, C., COLIN, C., BLAMART, D., FOUBERT, A., VAN ROOIJ, D., HENRIET, J. P., DE HAAS, H. & VAN WEERING, T. 2009. The Holocene occurrence of cold water corals in the NE Atlantic: implications for cor-al carbonate mound evolution. *Marine Geology,* 266(1-4), 129-142.

FREIWALD, A. 2002. Reef-forming cold-water corals. *In:* WEFER, G., BILLET, D., HEBBELN, D., JOR-GENSEN, B. B., SCHLÜTER, M. & WEERING, T. C. E. (eds.). *Ocean margin systems.* Berlin: Springer, pp. 365-385.

FREIWALD, A., FOSSÅ, J. H., GREHAN, A., KOSLOW, T. & ROBERTS, J. M. 2004. Cold-water coral reefs: out of sight - no longer out of mind. Cambridge: UNEP.

GISCHLER, E. & ZINGELER, D. 2016. The origin of car-bonate mud in isolated carbonate platforms of Belize, Central America. *International Journal of Earth Scienc-es,* 91, 1054-1070.

GOVIN, A., HOLZWARTH, U., HESLOP, D., KEELING, L. F., ZABEL, M., MULITZA, S., COLLINS, J. A. & CHIES-SI, C. M. 2012. Distribution of major elements in Atlantic surface sediments (36°N-49°S): imprint of terrigenous input and continental weathering. *Geochemistry, Geo-physics, Geosystems,* 13(1), 1-23.

GUERRA, M. C. M. & UNDERHILL, J. R. 2012. Role of halokinesis in controlling structural styles and sediment dispersal in the Santos Basin, offshore Brazil. *Geologi-cal Society, London, Special Publications,* 363, 175-206.

HAMMER, Ø., HARPER, D. A. T. & RYAN, P. D. 2001. PAST: Paleontological statistics software package for education and data analysis. *Palaeontologia Electroni-ca,* 4(1), 1-9.

HEATON, T. J., KÖHLER, P., BUTZIN, M., BARD, E., RE-IMER, R. W., AUSTIN, W. E. N., BRONK RAMSEY, C., GROOTES, P. M., HUGHEN, K. A., KROMER, B., RE-IMER, P. J., ADKINS, J., BURKE, A., COOK, M. S., OL-SEN, J. & SKINNER, L. C. 2020. Marine20—the marine radiocarbon age calibration curve (0-55,000 cal BP). *Radiocarbon,* 62(4), 779-820.

HENRIET, J. P., HAMOUMI, N., SILVA, A. C., FOUBERT, A., LAURIDSEN, B. W., RÜGGEBERG, A. & VAN ROOIJ, D. 2014. Carbonate mounds: from paradox to World Heritage. *Marine Geology,* 352, 89-110.

HOVLAND, M. 1990. Do carbonate reefs form due to fluid seepage? *Terra Nova,* 2(1), 8-18.

HOVLAND, M. 2008. North Atlantic coral reefs and giant carbonate mounds. *In:* HOVLAND, M. (ed.). *Deep-water coral reefs.* Dordrecht: Springer, pp. 103-139.

HUVENNE, V. A. I., BAILEY, W. R., SHANNON, P. M., NAETH, J., DI PRIMIO, R., HENRIET, J. P., HORS-FIELD, B., HAAS, H., WHEELER, A. & OLU-LE ROY, K. 2007. The Magellan mound province in the Porcu-pine Basin. *International Journal of Earth Sciences,* 96(1), 85-101.

JACKSON, C. A. L., JACKSON, M. P. A. & HUDEC, M. R. 2015. Understanding the kinematics of salt-bearing pas-sive margins: a critical test of competing hypotheses for the origin of the Albian Gap, Santos Basin, offshore Bra-zil. *Geological Society of America Bulletin,* 127(11-12), 1730-1751.

JACOBSEN, S. B. & WASSERBURG, G. J. 1980. Sm-Nd isotopic evolution of chondrites. *Earth and Planetary Science Letters,* 50(1), 139-155.

JOUBIN, L. 1922. Distribution géographique de quelques coraux abyssaux dans les mers occidentales européen-nes. *Comptes Rendus, Académie des Sciences,* 175, 930-933.

KANO, A., FERDELMAN, T. G., WILLIAMS, T., HENRIET, J. P., ISHIKAWA, T., KAWAGOE, N., TAKASHIMA, C., KAKIZAKI, Y., ABE, K., SAKAI, S., BROWNING, E. L. & LI, X. 2007. Age constraints on the origin and growth history of a deep-water coral mound in the northeast Atlantic drilled during Integrated Ocean Drilling Program Expedition 307. *Geology,* 35(11), 1051-1054.

KENYON, N. H., AKHMETZHANOV, A. M., WHEELER, A. J., VAN WEERING, T. C. E., HAAS, H. & IVANOV, M. K. 2003. Giant carbonate mud mounds in the southern Rockall Trough. *Marine Geology,* 195(1-4), 5-30.

LE GUILLOUX, E., OLU, K., BOURILLET, J. F., SAVOYE, B., IGLÉSIAS, S. P. & SIBUET, M. 2009. First observations of deep-sea coral reefs along the Angola margin. *Deep Sea Research Part II: Topical Studies in Oceanography,* 56(23), 2394-2403.

LEGEAIS, J. F., OLLITRAULT, M. & ARHAN, M. 2013. Lagrangian observations in the Intermediate Western Boundary Current of the South Atlantic. *Deep Sea Research Part II: Topical Studies in Oceanography,* 85, 109-126.

LINDHOLM-LEHTO, P., PULKKINEN, J., KIURU, T., KOSKELA, J. & VIELMA, J. 2020. Water quality in recirculating aquaculture system using woodchip denitrification and slow sand filtration. *Environmental Science and Pollution Research,* 27(14), 17314-17328.

MAGDALENO, G. B., PETRONILHO, L. A., RUIZ, I. R., BABINSKI, M., HOLLANDA, M. H. B. M. & MARTINS, V. T. S. 2017. Pb-Sr-Nd isotopoic characterization of USGS reference materials by TIMS at CPGeo-USP [online]. *In: II Workshop of inorganic mass spectrometry - 2017.* São Paulo: Institute of Geoscience of the University of São Paulo, pp. 1-3. Available at: https://wims.igc.usp.br/wp-content/uploads/2017/07/Giselle-Magdaleno.pdf [Accessed: 11 Oct. 2021].

MAHIQUES, M. M., HANEBUTH, T. J. J., NAGAI, R. H., BÍCEGO, M. C., FIGUEIRA, R. C. L., SOUSA, S. H. M., BURONE, L., FRANCO-FRAGUAS, P., TANIGUCHI, S., SALAROLI, A. B., DIAS, G. P., PRATES, D. M. & FREITAS, M. E. F. 2017. Inorganic and organic geochemical fingerprinting of sediment sources and ocean circulation on a complex continental margin (São Paulo Bight, Brazil). *Ocean Science,* 13, 209-222.

MAHIQUES, M. M., SCHATTNER, U., LAZAR, M., SUMIDA, P. Y. G. & SOUZA, L. A. P. 2017. An extensive pockmark field on the upper Atlantic margin of Southeast Brazil: spatial analysis and its relationship with salt diapirism. *Heliyon,* 3(2), e00257.

MAHIQUES, M. M., SOUSA, S. H. M., BURONE, L., NAGAI, R. H., SILVEIRA, I. C. A., SOUTELINO, R. G., PONSONI, L. & KLEIN, D. A. 2011. Radiocarbon geochronology of the sediments of the São Paulo Bight (Southern Brazilian upper margin). *Anais da Academia Brasileira de Ciências,* 83(3), 817-834.

MAHIQUES, M. M., TESSLER, M. G., CIOTTI, A. M., SILVEIRA, I. C. A., SOUSA, S. H. M., FIGUEIRA, R. C. L., TASSINARI, C. C. G., FURTADO, V. V. & PASSOS, R. F. 2004. Hydrodynamically driven patterns of recent sedimentation in the shelf and upper slope off Southeast Brazil. *Continental Shelf Research,* 24, 1685-1697.

MAHIQUES, M. M., VIOLANTE, R., FRANCO-FRAGUAS, P., BURONE, L., ROCHA, C. B., ORTEGA, L., SANTOS, R. F., MI KIM, B. S., FIGUEIRA, R. C. L. & BÍCEGO, M. C. 2021. Control of oceanic circulation on sediment distribution in the southwestern Atlantic margin (23 to 55° S). *Ocean Science,* 17, 1213-1229.

MOL, B., HUVENNE, V. & CANALS, M. 2008. Cold-water coral banks and submarine landslides: a review. *International Journal of Earth Sciences,* 98(4), 885-899.

MOL, B., VAN RENSBERGEN, P., PILLEN, S., VAN HERREWEGHE, K., VAN ROOIJ, D., MCDONNELL, A., HUVENNE, V., IVANOV, M., SWENNEN, R. & HENRIET, J. P. 2002. Large deep-water coral banks in the Porcupine Basin, southwest of Ireland. *Marine Geology,* 188(1-2), 193-231.

MALY, M., SCHATTNER, U., LOBO, F., RAMOS, R. B., DIAS, R. J., COUTO, D. M., SUMIDA, P. Y. & MAHIQUES, M. M. 2019. The Alpha Crucis Carbonate Ridge (ACCR): Discovery of a giant ring-shaped carbonate complex on the SW Atlantic margin. *Scientific Reports,* 9(1), 18697.

MANGELSDORF, K., ZINK, K. G., DI PRIMIO, R. & HORSFIELD, B. 2011. Microbial lipid markers within and adjacent to Challenger Mound in the Belgica carbonate mound province, Porcupine Basin, offshore Ireland (IODP Expedition 307). *Marine Geology,* 282(1), 91-101.

MANGINI, A., GODOY, J. M., GODOY, M. L., KOWSMANN, R., SANTOS, G. M., RUCKELSHAUSEN, M., SCHROEDER-RITZRAU, A. & WACKER, L. 2010. Deep sea corals off Brazil verify a poorly ventilated Southern Pacific Ocean during H2, H1 and the Younger Dryas. *Earth and Planetary Science Letters,* 293(3-4), 269-276.

MANTOVANELLI, S. S., TASSINARI, C. C. G., MAHIQUES, M. M., JOVANE, L. & BONGIOLO, E. 2018. Characterization of Nd radiogenic isotope signatures in sediments from the southwestern Atlantic Margin. *Frontiers in Earth Science,* 6, 74.

MARTINEZ-RUIZ, F., KASTNER, M., GALLEGO-TORRES, D., RODRIGO-GÁMIZ, M., NIETO-MORENO, V. & ORTEGA-HUERTAS, M. 2015. Paleoclimate and paleoceanography over the past 20,000 yr in the Mediterranean Sea Basins as indicated by sediment elemental proxies. *Quaternary Science Reviews,* 107, 25-46.

MIENIS, F., VAN DER LAND, C., STIGTER, H. C., VAN DE VORSTENBOSCH, M., DE HAAS, H., RICHTER, T. & VAN WEERING, T. C. E. 2009. Sediment accumulation on a cold-water carbonate mound at the Southwest Rockall Trough margin. *Marine Geology,* 265(1-2), 40-50.

MODICA, C. J. & BRUSH, E. R. 2004. Postrift sequence stratigraphy, paleogeography, and fill history of the deep-water Santos Basin, offshore southeast Brazil. *AAPG Bulletin,* 88, 923-945.

MOHRIAK, W. U., NEMČOK, M. & ENCISO, G. 2008. South Atlantic divergent margin evolution: rift-border uplift and salt tectonics in the basins of SE Brazil. *Geological Society, London, Special Publications,* 294(1), 365-398.

MORENO, A., CACHO, I., CANALS, M., GRIMALT, J. O. & SANCHEZ-VIDAL, A. 2004. Millennial-scale variability in the productivity signal from the Alboran Sea record, Western Mediterranean Sea. *Palaeogeography, Palaeoclimatology, Palaeoecology,* 211(3), 205-219.

MORFORD, J. L., RUSSELL, A. D. & EMERSON, S. 2001. Trace metal evidence for changes in the redox environment associated with the transition from terrigenous clay to diatomaceous sediment, Saanich Inlet, BC. *Marine Geology,* 174(1-4), 355-369.

MORIGI, C., SABBATINI, A., VITALE, G., PANCOTTI, I., GOODAY, A. J., DUINEVELD, G. C. A., DE STIGTER, H. C., DANOVARO, R. & NEGRI, A. 2012. Foraminiferal biodiversity associated with cold-water coral carbonate mounds and open slope of SE Rockall Bank (Irish continental margin—NE Atlantic). *Deep Sea Research Part I: Oceanographic Research Papers,* 59, 54-71.

NAMEROFF, T. J., CALVERT, S. E. & MURRAY, J. W. 2004. Glacial-interglacial variability in the eastern tropical North Pacific oxygen minimum zone recorded by redox-sensitive trace metals. *Paleoceanography,* 19(1), 1-54.

NEUMANN, A. C., KOFOED, J. W. & KELLER, G. H. 1977. Lithoherms in the Straits of Florida. *Geology,* 5(1), 4-10.

NUNES, M. C. V., VIVIERS, M. C. & LANA, C. C. 2004. *Bacias Sedimentares Brasileiras, Bacia de Santos.* Aracaju: Fundação Paleontológica Phoenix.

PERASSOLI, F., GHISOLFI, R. D. & LEMOS, A. T. 2020. Spatial distribution of nutrients associated with water masses in the Tubarão Bight (20°S-22°S), Brazil. *Journal of Marine Systems,* 212, 103425.

PIOLA, A. R., MATANO, R. P., PALMA, E. D., MÖLLER, O. O. & CAMPOS, E. J. D. 2005. The influence of the Plata River discharge on the western South Atlantic shelf. *Geophysical Research Letters,* 32, L01603.

PIRLET, H., COLIN, C., THIERENS, M., LATRUWE, K., VAN ROOIJ, D., FOUBERT, A., FRANK, N., BLAMART, D., HUVENNE, V. A. I., SWENNEN, R., VANHAECKE, F. & HENRIET, J. P. 2011. The importance of the terrigenous fraction within a cold-water coral mound: A case study. *Marine Geology,* 282(1-2), 13-25.

POREVSKY, P. Á., RUIZ, H. G. & RUIZ, H. G. 2014. Comparison of Soxhlet extraction, ultrasonic bath and focused microwave extraction techniques for the simultaneous extraction of PAH´s and pesticides from sediment samples. *Scientia Chromatographica,* 6(2), 124-138.

PORTILHO-RAMOS, R. C., CRUZ, A. P. S., BARBOSA, C. F., RATHBURN, A. E., MULITZA, S., VENANCIO, I. M., SCHWENK, T., RUHLEMANN, C., VIDAL, L., CHIESSI, C. M. & SILVEIRA, C. S. 2018. Methane release from the southern Brazilian margin during the last glacial. *Scientific Reports,* 8(1), 5948.

RADDATZ, J., TITSCHACK, J., FRANK, N., FREIWALD, A., CONFORTI, A., OSBORNE, A., SKORNITZKE, S., STILLER, W., RÜGGEBERG, A., VOIGT, S., ALBUQUERQUE, A. L. S., VERTINO, A., SCHRÖDER-RITZRAU, A. & BAHR, A. 2019. Solenosmilia variabilis-bearing cold-water coral mounds off Brazil. *Coral Reefs,* 39, 69-83.

RAZIK, S., GOVIN, A., CHIESSI, C. M. & VON DOBENECK, T. 2015. Depositional provinces, dispersal, and origin of terrigenous sediments along the SE South American continental margin. *Marine Geology,* 363, 261-272.

RICHTER, T. O., VAN DER GAAST, S., KOSTER, B., VAARS, A., GIELES, R., DE STIGTER, H. C., DE HAAS, H. & VAN WEERING, T. C. E. 2006. The Avaatech XRF Core Scanner: technical description and applications to NE Atlantic sediments. *Geological Society, London, Special Publications,* 267, 39-50.

ROBERTS, J. M., WHEELER, A. J. & FREIWALD, A. 2006. Reefs of the deep: the biology and geology of cold-water coral ecosystems. *Science,* 312(5773), 543-547.

ROTHWELL, R. G. & CROUDACE, I. W. 2015. Twenty years of XRF core scanning marine sediments: what do geochemical proxies tell us? *In:* CROUDACE, I. W. & ROTHWELL, R. G. (eds.). *Micro-XRF studies of sediment cores.* Dordrecht: Springer, pp. 25-102.

RÜGGEBERG, A., DORSCHEL, B., DULLO, W. C. & HEBBELN, D. 2005. Sedimentary patterns in the vicinity of a carbonate mound in the Hovland Mound Province, northern Porcupine Seabight. *In:* FREIWALD, A. & ROBERTS, J. M. (eds.). *Cold-water corals and ecosystems.* Berlin: Springer, pp. 87-112.

RÜGGEBERG, A., DULLO, W. C., DORSCHEL, B. & HEBBELN, D. 2007. Environmental changes and growth history of a cold-water carbonate mound (Propeller Mound, Porcupine Seabight). *International Journal of Earth Sciences,* 96(1), 57-72.

SANTOS, R. F., NAGAOKA, D., RAMOS, R. B., SALAROLI, A. B., TANIGUCHI, S., FIGUEIRA, R. C. L., BÍCEGO, M. C., LOBO, F. J., SCHATTNER, U. & MAHIQUES, M. M. 2018. Metal/Ca ratios in pockmarks and adjacent sediments on the SW Atlantic slope: Implications for redox potential and modern seepage. *Journal of Geochemical Exploration,* 192, 163-173.

SATO, K., TASSINARI, C. C. G., KAWASHITA, K. & PETRONILHO, L. 1995. A metodologia Sm-Nd no IGc--USP e suas aplicações. *Anais da Academia Brasileira de Ciências,* 67(3), 313-336.

SCHATTNER, U., LAZAR, M., SOUZA, L. A. P., TEN BRINK, U. & MAHIQUES, M. M. 2016. Pockmark asymmetry and seafloor currents in the Santos Basin offshore Brazil. *Geo-Marine Letters,* 36, 457-464.

SCHATTNER, U., LOBO, F. J., GARCÍA, M., KANARI, M., RAMOS, R. B. & MAHIQUES, M. M. 2018. A detailed look at diapir piercement onto the ocean floor: new evidence from Santos Basin, offshore Brazil. *Marine Geology,* 406, 98-108.

SCHATTNER, U., LOBO, F. J., LÓPEZ-QUIRÓS, A., PASSOS NASCIMENTO, J. L. & MAHIQUES, M. M. 2020. What feeds shelf-edge clinoforms over margins deprived of adjacent land sources? An example from Southeastern Brazil. *Basin Research,* 32(2), 293-301.

SILVEIRA, I. C. A., CALADO, L., CASTRO, B. M., CIRANO, M., LIMA, J. A. M. & MASCARENHAS, A. D. S. 2004. On the baroclinic structure of the Brazil current-intermediate Western Boundary Current system at 22°-23°S. *Geophysical Research Letters,* 31(14), L14308.

SOUZA, R. B. & ROBINSON, I. S. 2004. Lagrangian and satellite observations of the Brazilian Coastal Current. *Continental Shelf Research,* 24, 241-262.

STEINMANN, L., BAQUES, M., WENAU, S., SCHWENK, T., SPIESS, V., PIOLA, A. R., BOZZANO, G., VIOLANTE, R. & KASTEN, S. 2020. Discovery of a giant cold-water coral mound province along the northern Argentine margin and its link to the regional Contourite Depositional System and oceanographic setting. *Marine Geology,* 427, 106223.

STUIVER, M., REIMER, P. J. & REIMER, R. W. 2021. *CALIB 8.2 radiocarbon calibration* [online]. Cambridge: Radiocarbon - CALIB Program. Available at: http://calib.org/calib/ [Accessed: 2020 Nov 11].

SUESS, E. 2014. Marine cold seeps and their manifestations: geological control, biogeochemical criteria and environmental conditions. *International Journal of Earth Sciences,* 103, 1889-1916.

SUMIDA, P. Y. G., YOSHINAGA, M. Y., MADUREIRA, L. A. S. P. & HOVLAND, M. 2004. Seabed pockmarks associated with deepwater corals off SE Brazilian continental slope, Santos Basin. *Marine Geology,* 207, 159-167.

SUZUKI, M. S., REZENDE, C. E., PARANHOS, R. & FALCÃO, A. P. 2015. Spatial distribution (vertical and horizontal) and partitioning of dissolved and particulate nutrients (C, N and P) in the Campos Basin, Southern Brazil. *Estuarine, Coastal and Shelf Science,* 166, 4-12.

TEICHERT, C. 1958. Cold- and deep-water coral banks. *AAPG Bulletin,* 42(5), 1064-1082.

TERHZAZ, L., HAMOUMI, N., SPEZZAFERRI, S., LOTFI, E. M. & HENRIET, J. P. 2018. Carbonate mounds of the Moroccan Mediterranean margin: Facies and environmental controls. *Comptes Rendus Geoscience,* 350(5), 212-221.

THIAGARAJAN, N., GERLACH, D., ROBERTS, M. L., BURKE, A., MCNICHOL, A., JENKINS, W. J., SUBHAS, A. V., THRESHER, R. E. & ADKINS, J. F. 2013. Movement of deep-sea coral populations on climatic timescales. *Paleoceanography,* 28, 227-236.

THIERENS, M., TITSCHACK, J., DORSCHEL, B., HUVENNE, V. A. I., WHEELER, A. J., STUUT, J. B. & O'DONNELL, R. 2010. The 2.6Ma depositional sequence from the Challenger cold-water coral carbonate mound (IODP Exp. 307): sediment contributors and hydrodynamic palaeo-environments. *Marine Geology,* 271(3-4), 260-277.

TITSCHACK, J., THIERENS, M., DORSCHEL, B., SCHULBERT, C., FREIWALD, A., KANO, A., TAKASHIMA, C., KAWAGOE, N. & LI, X. 2009. Carbonate budget of a cold-water coral mound (Challenger Mound, IODP Exp. 307). *Marine Geology,* 259, 36-46.

TRIBOVILLARD, N. 2021. Re-assessing copper and nickel enrichments as paleo-productivity proxies. *BSGF - Earth Sciences Bulletin,* 192, 54.

TRIBOVILLARD, N., ALGEO, T. J., LYONS, T. & RIBOULLEAU, A. 2006. Trace metals as paleoredox and paleoproductivity proxies: an update. *Chemical Geology,* 232(1-2), 12-32.

USEPA (U.S. Environmental Protection Agency). 1996. *Method 3052. Microwave assisted acid digestion of siliceous and organically based matrices* [online]. Washington: USEPA. Available at: https://www.epa.gov/sites/production/files/2015-12/documents/3052.pdf [Accessed: 2020 April 28].

VAN DER LAND, C., EISELE, M., MIENIS, F., DE HAAS, H., HEBBELN, D., REIJMER, J. J. G. & VAN WEERING, T. C. E. 2014. Carbonate mound development in contrasting settings on the Irish margin. *Deep Sea Research Part II: Topical Studies in Oceanography,* 99, 297-306.

VAN DER LAND, C., MIENIS, F., HAAS, H., STIGTER, H. C., SWENNEN, R., REIJMER, J. J. G. & VAN WEERING, T. C. E. 2011. Paleo-redox fronts and their formation in carbonate mound sediments from the Rockall Trough. *Marine Geology,* 284, 86-95.

VAN WEERING, T. C. E., DE HAAS, H., DE STIGTER, H. C., LYKKE-ANDERSEN, H. & KOUVAEV, I. 2003. Structure and development of giant carbonate mounds at the SW and SE Rockall Trough margins, NE Atlantic Ocean. *Marine Geology,* 198(1), 67-81.

VIANA, A. R., FAUGERES, J. C., KOWSMANN, R. O., LIMA, J. A. M., CADDAH, L. F. G. & RIZZO, J. G. 1998. Hydrology, morphology and sedimentology of the Campos continental margin, offshore Brazil. *Sedimentary Geology,* 115(1-4), 133-157.

WAGREICH, M. & KOUKAL, V. 2020. The pelagic archive of short-term sea-level change in the Cretaceous: a review of proxies linked to orbital forcing. *Geological Society, London, Special Publications,* 498, 39-56.

WELTJE, G. J. 1997. End-member modeling of compositional data: Numerical-statistical algorithms for solving the explicit mixing problem. *Mathematical Geology,* 29, 503-549.

WHEELER, A. J., BEYER, A., FREIWALD, A., DE HAAS, H., HUVENNE, V. A. I., KOZACHENKO, M., OLU-LE ROY, K. & OPDERBECKE, J. 2006. Morphology and environment of cold-water coral carbonate mounds on the NW European margin. *International Journal of Earth Sciences,* 96, 37-56.

WHITE, M. 2006. Benthic dynamics at the carbonate mound regions of the Porcupine Sea Bight continental margin. *International Journal of Earth Sciences,* 96(1), 1-9.

WHITE, M. & DORSCHEL, B. 2010. The importance of the permanent thermocline to the cold water coral carbonate mound distribution in the NE Atlantic. *Earth and Planetary Science Letters,* 296(3-4), 395-402.

ZEMBRUSCKI, S. G. 1979. Geomorfologia da margem continental sul brasileira e das bacias oceânicas adjacentes. *In:* CHAVES, H. A. F. (ed.). *Geomorfologia da margem continental Brasileira e áreas oceânicas adjacentes.* Rio de Janeiro: Petrobrás, pp. 129-177.

ZHANG, X., WANG, H., XU, S. & YANG, Z. 2020. A basic end-member model algorithm for grain-size data of marine sediments. *Estuarine, Coastal and Shelf Science,* 236, 106656.